Cell PRESS
Neuron
Report

BLA to vHPC Inputs Modulate Anxiety-Related Behaviors

Ada C. Felix-Ortiz,[1,2] Anna Beyeler,[1,2] Changwoo Seo,[1] Christopher A. Leppla,[1] Craig P. Wildes,[1] and Kay M. Tye[1,*]
[1]The Picower Institute for Learning and Memory, Department of Brain & Cognitive Sciences, Massachusetts Institute of Technology, Cambridge, MA 02139, USA
[2]These authors contributed equally to this work
*Correspondence: kaytye@mit.edu
http://dx.doi.org/10.1016/j.neuron.2013.06.016

SUMMARY

The basolateral amygdala (BLA) and ventral hippocampus (vHPC) have both been implicated in mediating anxiety-related behaviors, but the functional contribution of BLA inputs to the vHPC has never been directly investigated. Here we show that activation of BLA-vHPC synapses acutely and robustly increased anxiety-related behaviors, while inhibition of BLA-vHPC synapses decreased anxiety-related behaviors. We combined optogenetic approaches with in vivo pharmacological manipulations and ex vivo whole-cell patch-clamp recordings to dissect the local circuit mechanisms, demonstrating that activation of BLA terminals in the vHPC provided monosynaptic, glutamatergic inputs to vHPC pyramidal neurons. Furthermore, BLA inputs exerted polysynaptic, inhibitory effects mediated by local interneurons in the vHPC that may serve to balance the circuit locally. These data establish a role for BLA-vHPC synapses in bidirectionally controlling anxiety-related behaviors in an immediate, yet reversible, manner and a model for the local circuit mechanism of BLA inputs in the vHPC.

INTRODUCTION

Although amygdala circuitry has been implicated in anxiety in both humans (Büchel et al., 1999; Etkin et al., 2009; Somerville et al., 2004) and rodent models (Adamec et al., 1999; Davidson, 2002), the way in which it interacts with a distributed neural circuit to mediate anxiety is poorly understood. In rodents, a causal role for the amygdala microcircuitry has emerged in fear and anxiety (Ciocchi et al., 2010; Han et al., 2009; Haubensak et al., 2010; Tye et al., 2011), but relationships between the amygdala and distal regions are still unclear.

One distal amygdalar projection target implicated in anxiety-related behaviors is the ventral hippocampus (vHPC; File and Gonzalez, 1996; McHugh et al., 2004; Richardson et al., 2004). The vHPC shares robust reciprocal connections with the basolateral nucleus of the amygdala (BLA; O'Donnell and Grace, 1995; Pikkarainen et al., 1999). Subsequent studies have concluded that the ventral, but not the dorsal, hippocampus is required for the expression of anxiety-related behaviors in the elevated plus maze (EPM) and open-field test (OFT) (Bannerman et al., 2003; Kheirbek et al., 2013; Kjelstrup et al., 2002). In vivo electrophysiology recordings have revealed neural correlates in the BLA and vHPC to anxiety-related behaviors, such as increased tonic firing in BLA (Wang et al., 2011) and increased theta-frequency synchrony between the vHPC and prefrontal cortex (PFC; Adhikari et al., 2010, 2011). Although these studies establish neural correlates between anxiety-related behaviors and the BLA or vHPC during anxiety assays, the precise neural encoding dynamics of the BLA-vHPC projection are unknown.

Our recent work demonstrated that activation of BLA somata produced opposing effects on anxiety-related behaviors than activation of BLA projections to the central nucleus of the amygdala (CeA; Tye et al., 2011). Given that BLA neurons project to many different downstream targets (Pikkarainen et al., 1999; Pitkänen et al., 1995), and mediate many different behaviors (Paton et al., 2006; Tye et al., 2010), this result raised the possibility that different projection targets could mediate opposing effects on anxiety-related behaviors. Perhaps BLA projections to the CeA only represented a minority of effects, and nonspecific activation of BLA neurons to all targets yielded a net effect of increased anxiety. To test this hypothesis and explore the function of distal projections from the BLA to the vHPC, we leveraged the power of optogenetic projection-specific manipulations (Tye and Deisseroth, 2012) in freely moving rodents. Here, we identify a functional role for the BLA-vHPC pathway in bidirectionally and reversibly modulating anxiety-related behaviors and elucidate the synaptic mechanisms of BLA inputs to the vHPC.

RESULTS

Optogenetic Inhibition of BLA Inputs to the vHPC Reduces Anxiety-Related Behaviors

We expressed an enhanced version of halorhodopsin (NpHR is an abbreviation for eNpHR3.0; Gradinaru et al., 2010) in BLA pyramidal neurons using an adeno-associated viral vector serotype 5 (AAV_5) under the control of the CaMKIIα promoter. BLA projection neurons were transduced with NpHR fused to an enhanced yellow fluorescent protein (eYFP) in experimental animals (AAV_5-CaMKIIα-NpHR-eYFP), while control animals matched for age, incubation time, and illumination parameters received the same viral vector carrying the fluorophore alone

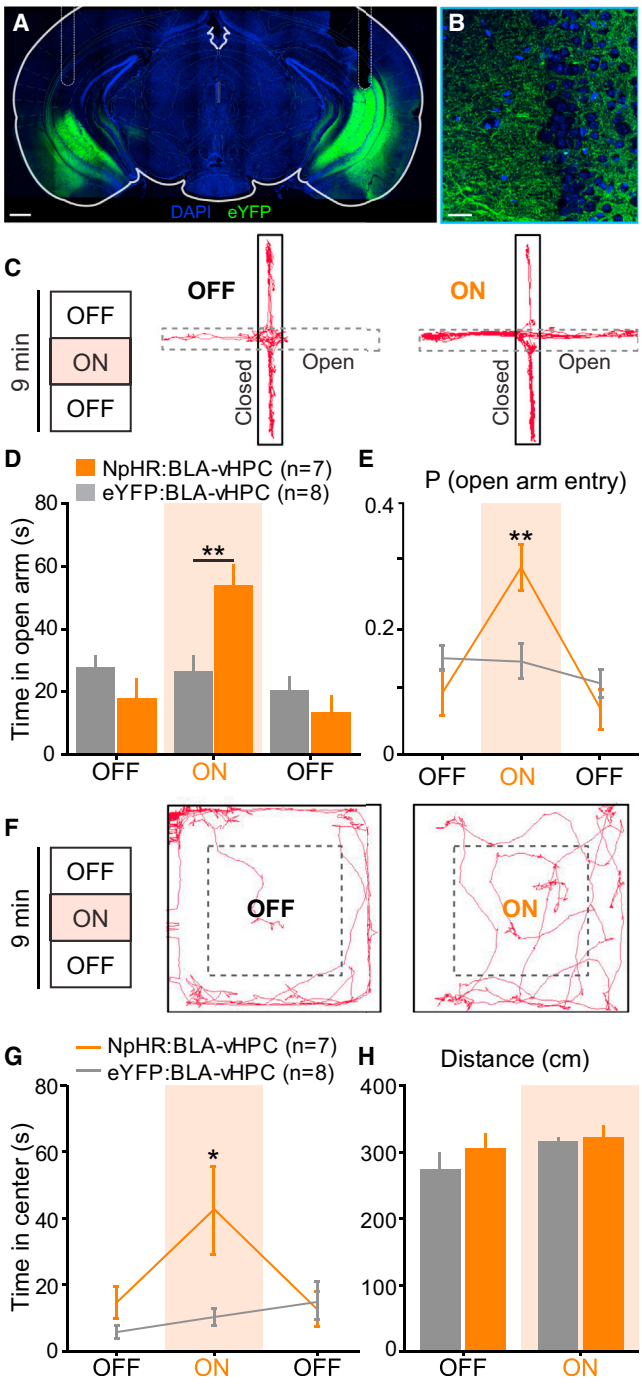

Figure 1. Inhibition of BLA Projections to vHPC with NpHR Decreases Anxiety-Related Behaviors

Glutamatergic neurons in the BLA were transduced with either NpHR-eYFP (n = 7 mice) or eYFP (n = 8 mice). Yellow light was delivered (3 min, constant) via bilateral optical fibers implanted in the vHPC, after ~6 weeks of viral incubation. Means are represented as ±SEM. See also Figures S1 and S2 and Movie S1. (A) Confocal image of a coronal section containing the vHPC, from an NpHR:BLA-vHPC mouse. Scale bar represents 150 μm. (B) Overlay magnification of BLA terminals on the vHPC (DAPI in blue and eYFP in green). Scale bar represents 50 μm. (C) Representative animal track for the first two epochs of EPM for an NpHR-mouse. Left: 3 min epochs across the 9 min session. (D) NpHR-mice spent significantly more time in the open arms than eYFP-mice during the illumination epoch (two-way ANOVA group × epoch interaction, $F_{2,26} = 14.09$, $p = 0.0001$; Bonferroni post hoc analysis,**$p < 0.01$). (E) NpHR-mice showed a significantly higher probability of open-arm entry than eYFP-mice (two-way ANOVA group × epoch interaction, $F_{2,26} = 10.17$, $p = 0.0005$; Bonferroni post hoc analysis,**$p < 0.01$). (F) Representative animal track in the open-field chamber for an NpHR mouse. (G) During illumination, NpHR-mice spent significantly more time in the center than eYFP-mice (two-way ANOVA group × epoch interaction, $F_{2,26} = 10.17$, $p = 0.0005$; Bonferroni post hoc analysis, **$p < 0.01$). (H) No effect of light stimulation or group was detected on the traveled distance (two-way ANOVA group × epoch interaction, $F_{2,26} = 0.56$, $p = 0.4685$).

(AAV_5-CaMKIIα-eYFP). To inhibit NpHR-expressing BLA axon terminals in the vHPC, we bilaterally implanted optical fibers above the vHPC to allow for the delivery of amber (594 nm) light to the pyramidal layer of the vHPC (Figures 1A, 1B, and S1 available online). To investigate the functional contribution of BLA inputs to the vHPC, we probed freely moving mice under projection-specific optogenetic control on two well-validated anxiety assays (Carola et al., 2002), the EPM and the OFT. To allow for within-subject and within-session comparisons in addition to group comparisons, we tested mice on a single 9 min session on both the EPM and OFT with three 3 min epochs, beginning with a light-off (OFF) baseline epoch, followed by a light-on (ON) illumination epoch using constant illumination with 594 nm light, alternating back to a second OFF epoch. A representative EPM animal track from the NpHR group is shown during the baseline OFF epoch and the ON epoch (Figure 1C). Mice in the NpHR group showed significantly greater open-arm exploration, reflecting a reduction in anxiety-related behaviors, relative to eYFP mice during the ON epoch (Figure 1D). Mice in the NpHR group also displayed an increased probability of open-arm entry during the ON epoch (Figure 1E). Because of the limitations of the EPM, wherein anxiogenic effects restrict exploration to the confinement of the closed arms, we also tested mice on the OFT where we could simultaneously assay anxiety-related behaviors and locomotion.

Using the same illumination parameters as on the EPM, a representative animal track from the NpHR group is shown for the baseline OFF epoch and the ON epoch (Figure 1F). Consistent with our EPM results, NpHR mice showed an increase in center exploration reflecting an anxiolytic effect upon illumination in the ON epoch relative to eYFP control mice (Figure 1G). Importantly, we did not detect an effect of light in the NpHR group on locomotion, as measured by distance traveled (Figure 1H) or ambulation velocity (Figure S2A). These data demonstrate that inhibiting BLA inputs to the vHPC robustly and reversibly induces an anxiolytic effect on the order of seconds. Next, we explored whether the ability of BLA inputs to the vHPC could control anxiety in a bidirectional manner.

Optogenetic Activation of BLA-vHPC Projections Increases Anxiety-Related Behaviors

To test whether activation of BLA axons in the vHPC was sufficient to cause an increase in anxiety-related behaviors, we expressed a channelrhodopsin-2 (ChR2)-eYFP fusion protein in BLA pyramidal neurons in experimental animals (Figures 2A and S3) and eYFP alone in control animals along with a

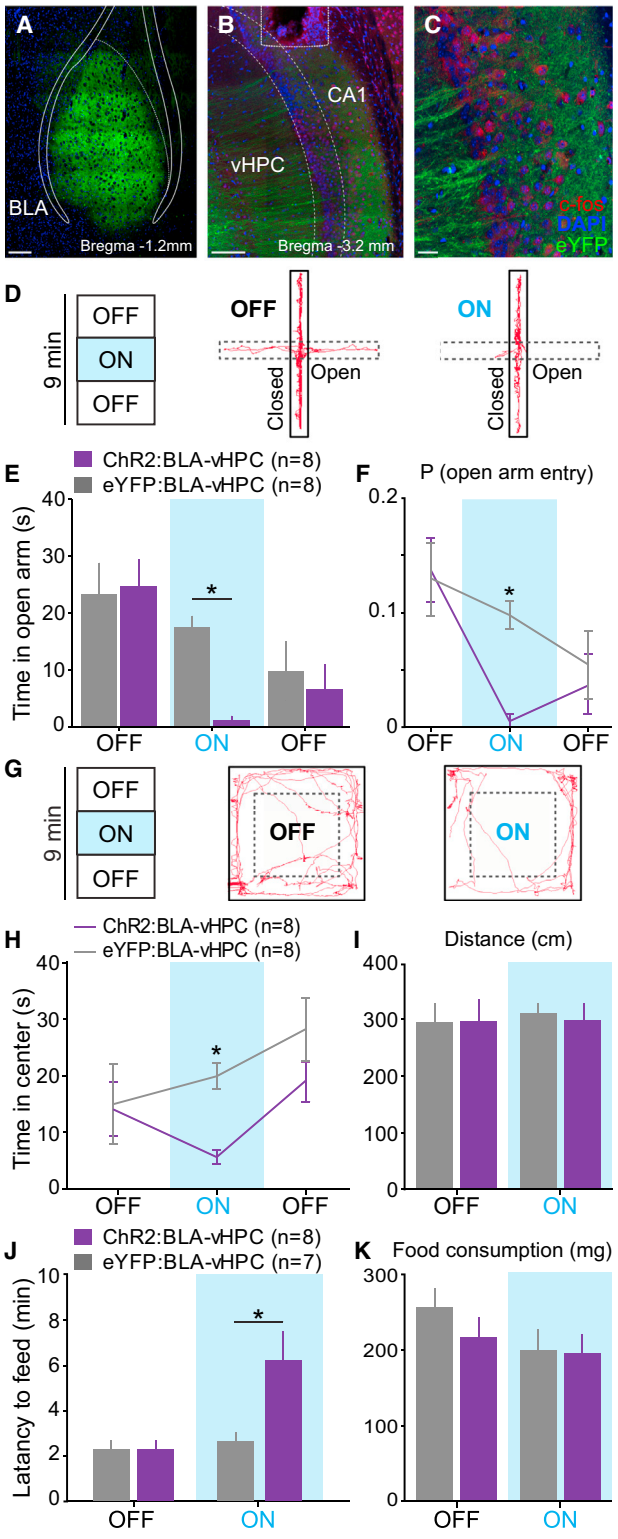

Figure 2. Activation of BLA Projections to the vHPC Increases Anxiety-Related Behaviors

BLA neurons were transduced with ChR2 (n = 8 mice) or eYFP (n = 8 mice). Blue light was delivered (20 Hz, 5 ms pulses) via a unilateral optical fiber implanted over the vHPC. Means are represented as ±SEM. See also Figures S2–S5 and Movie S2. (A–C) Confocal images of coronal sections from a ChR2-mouse, containing the BLA in (A), CA1 subregion of the vHPC in (B), and a magnified overlay of BLA terminals in the vHPC (*c-fos* in red, DAPI in blue, and eYFP in green) (C). Scale bars represent 150 μm for (A) and (B) and 50 μm for (C). (D) EPM tracks for a representative ChR2-mouse during the first two epochs (OFF and ON). (E) During the illumination epoch (ON), ChR2-mice spent significantly less time in the open arms, relative to eYFP-mice during photostimulation (two-way ANOVA group × epoch interaction, $F_{2,28} = 8.13$, $p = 0.0016$; Bonferroni post hoc analysis, *$p < 0.05$). (F) ChR2-mice showed a significantly lower probability of entering open arms, relative to eYFP-mice (two-way ANOVA group × epoch interaction, $F_{2,28} = 6.11$, $p = 0.0063$; Bonferroni post hoc analysis, *$p < 0.05$). (G) Representative animal tracks on OFT during the first two epochs for a ChR2-mouse. (H) During the illumination epoch, ChR2-mice spent significantly less time exploring the center of the open field than eYFP-mice (two-way ANOVA group × epoch interaction, $F_{2,28} = 5.23$, $p = 0.0118$; Bonferroni post hoc analysis, *$p < 0.05$). (I) Photostimulation did not alter the distance traveled for either group (two-way ANOVA did not detect a group × epoch interaction, $F_{1,14} = 0.09$, $p = 0.7669$). (J) Illumination significantly increased the latency to feed in a novel environment (two-way ANOVA group × epoch interaction, $F_{1,13} = 6.28$, $p = 0.0263$;Bonferroni post hoc analysis, *$p < 0.05$). (K) Food consumption during NSF was not altered by the group or the light stimulation (two-way ANOVA did not detect a group × epoch interaction, $F_{1,13} = 0.65$, $p = 0.4330$).

unilaterally implanted optical fiber over the vHPC on the ipsilateral hemisphere (Figures 2B, 2C, and S3) prior to testing on anxiety assays (Figures 2D–2K). We used the same 9 min session with alternating OFF-ON-OFF epochs as in the previous experiments but with the illumination epoch consisting of a continuous train at 20 Hz of blue (473 nm) light pulses, with a 5 ms pulse duration. A representative animal track from the ChR2 group is shown (Figure 2D), along with population data showing that animals in the ChR2 group showed reduced open-arm exploration during the ON epoch relative to eYFP controls (Figure 2E), as well as a lower probability of open-arm entry (Figure 2F). To evaluate the ability of BLA-vHPC projection activation to modulate anxiety-related behaviors or locomotor activity, we tested these animals on the OFT, for which a representative animal track from the ChR2 group is shown (Figure 2G). Mice in the ChR2 group displayed a decrease in center exploration time upon illumination during the ON epoch relative to eYFP controls (Figure 2H). Again, we simultaneously assayed locomotor activity across epochs and did not detect any changes during the ON epoch relative to the baseline OFF epoch in locomotion as measured by distance traveled (Figure 2I), velocity (Figure S2B), or freezing (Figure S2C).

To confirm the notion that the vHPC is thought to be involved in anxiety, but not spatial learning (Bannerman et al., 2003; Kheirbek et al., 2013), we investigated optogenetic manipulation of the BLA-vHPC pathway in an anxiety assay independent of exploration. Indeed, we replicated our EPM and OFT results in the novelty-suppressed feeding (NSF) test and found a greater latency to feed upon illumination of BLA terminals in the vHPC in the ChR2 group relative to both eYFP controls or baseline (OFF) conditions (Figure 2J), without an alteration in food consumption (Figure 2K) or body weight (Figures S2E and S2F).

To empirically determine the functional penetrance of blue light through brain tissue in terms of neuronal activation, and to test whether we could observe an increase in vHPC activity after illumination, we used the immediate early gene c-*fos* as a

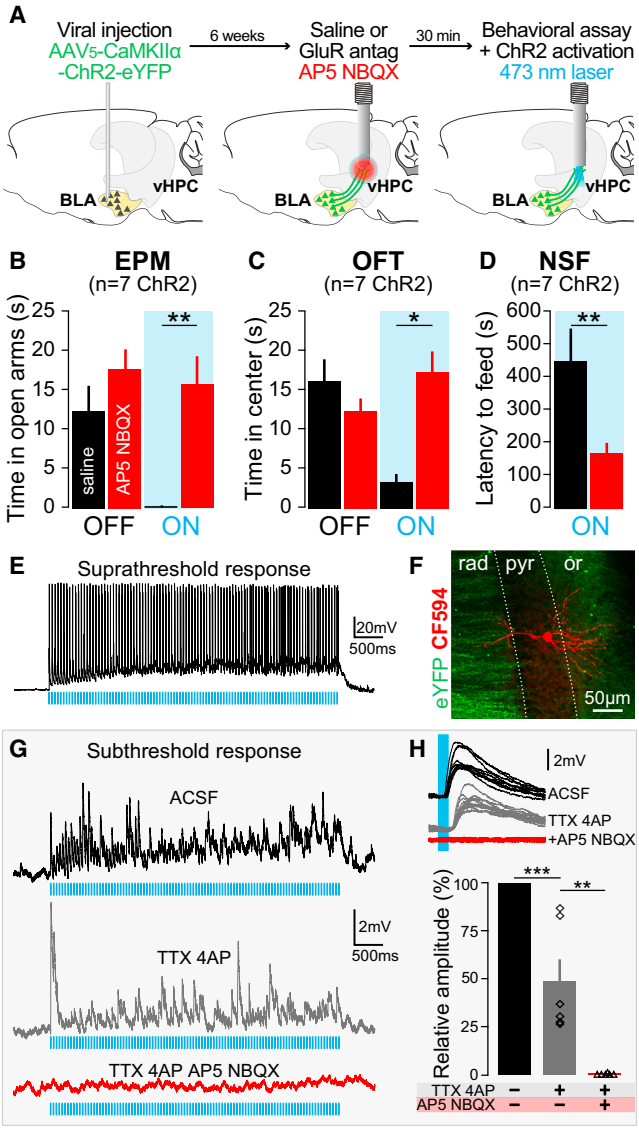

Figure 3. Monosynaptic and Glutamatergic BLA Inputs to the vHPC Are Sufficient to Mediate Changes in Anxiety-Related Behaviors

Experiments were performed 6–7 weeks after AAV_5-CaMKIIα-ChR2-eYFP injections in the BLA. Means are represented as ±SEM. See also Figures S6–S8. (A) Thirty minutes before behavioral assays and laser stimulation, glutamate receptor antagonists (GluR antag: AP5+NBQX, red) or saline (black) were unilaterally infused locally into the vHPC using the same guide cannula to be used for light delivery via an optical fiber. (B–D) Unilateral AP5+NBQX injection in the vHPC significantly attenuated light-induced increases in anxiety-related behaviors in the EPM, OFT, and NSF relative to saline trials. (B) Intra-vHPC GluR antag microinjection in mice expressing ChR2 in BLA axon terminals blocked the light-induced decrease of open-arm exploration (two-way ANOVA group × light epoch interaction $F_{2,24} = 7.35$, $p = 0.0032$); Bonferroni post hoc analyses showed that mice spent significantly more time in the open arm during light stimulation after intra-vHPC glutamate receptor antagonism (**$p < 0.01$), but unilateral GluR antag injection did not affect the basal level of open-arm exploration ($p > 0.05$). (C) After unilateral intra-vHPC glutamate receptor blockade, photoactivation of ChR2-expressing BLA terminals in the vHPC failed to decrease center exploration as seen after saline-treatment trials (two-way ANOVA, $F_{2,24} = 4.17$, $p = 0.0279$, Bonferroni post hoc, *$p < 0.05$). GluR antag injection did not affect the basal level of open-arm exploration ($p > 0.05$). (D) GluR antag injection into the vHPC attenuated light-induced increase of latency to feed as seen after saline treatment (one-tailed, paired Student's t test, n = 7, t = 3.24, **p = 0.0088). (E) Suprathreshold response to photostimulation (20 Hz, 5 ms pulses) of a CA1-vHPC neuron recorded ex vivo in the pyramidal layer (current clamp). (F) Confocal image of a neuron recorded, filled with biocytin and visualized by streptavidin-CF594 reaction (red). Inputs coming from BLA transfected neurons (eYFP). Dotted lines represent the borders of CA1 pyramidal layer (pyr) surrounded by the stratum oriens (or) and stratum radiatum (rad). (G) Subthreshold response of a CA1-vHPC neuron to photostimulation (ACSF, black, 20 Hz, 5 ms pulses). Photoresponse remains after the application of sodium and potassium channel blockers (TTX+4AP, gray) and is abolished by application of GluR antag (TTX+4AP+AP5+NBQX, red). (H) Overlay of ten responses evoked by 5 ms light pulses (ACSF, black), under TTX+4AP perfusion (gray), and after addition of GluR antag (TTX+AP4+NBQX+AP5, red). Histogram population analysis of light-induced EPSP amplitudes confirm that photo-induced EPSP persists after TTX+4AP perfusion (one-way ANOVA, $F_{2,10} = 53.71$, ***$p < 0.001$, Tukey post hoc analysis, ***$p < 0.001$) and are abolished after application of GluR antag (Tukey post hoc analysis, **$p < 0.01$).

readout for neural activity. Although we did not observe a change in BLA somata c-*fos* expression induced by illumination of BLA terminals in the vHPC, c-*fos* expression was increased in the pyramidal layer of the vHPC extending to ~1.5 mm below the fiber tip (Figures S4 and S5). We complemented our c-*fos* readouts with estimated irradiance levels through brain tissue using an empirically based model and illumination during whole-cell patch-clamp recordings (see Supplemental Experimental Procedures).

While these data indicate that inhibition of BLA terminals in the vHPC can reduce anxiety-related behaviors, the illumination of ChR2-expressing processes in the vHPC could carry the potential for inducing backpropagating action potentials (Petreanu et al., 2007) or depolarization of axons of passage. To test whether the activation of BLA axon terminals synapsing locally in the vHPC was the underlying mechanism of this light-induced change in anxiety-related behavior, we combined in vivo pharmacological manipulations with our in vivo optogenetic manipulations during anxiety assays (Figures 3A–3D).

BLA-vHPC Excitatory Synapses Are Sufficient to Mediate Changes in Anxiety-Related Behaviors

To determine whether the robust changes in anxiety-related behaviors that we observed were indeed mediated by monosynaptic, glutamatergic inputs from the BLA to the vHPC, rather than axons of passage or antidromic activation of BLA somata, we performed an additional series of experiments (Figure 3). First, we expressed ChR2 in BLA projection neurons as before and implanted a guide cannula to deliver either saline or glutamate receptor antagonists to the vHPC 30 min prior to testing and illumination on the EPM, OFT, or NSF (Figures 3A and S6). To allow for a within-subject comparison, we tested each animal twice on different days and contexts administering either saline or a glutamate receptor antagonist cocktail, counterbalanced for order. We compared saline trials to trials in which the combination of AMPA and NMDA receptor antagonists, 2,3-dihydroxy-6-nitro-7-sulfamoyl-benzo[f]quinoxaline-2,3-dione (NBQX) and (2R)-amino-5-phosphono-pentanoate (AP5), respectively, was intracranially administered to the vHPC. In saline trials, mice replicated the light-induced anxiogenic effect on both the EPM

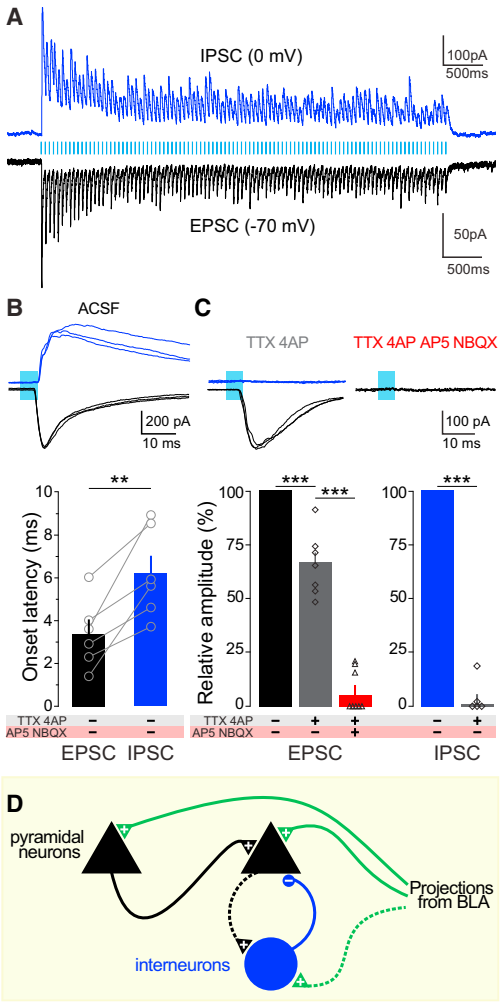

Figure 4. Local Circuit Mechanism Involves Direct Excitation and Indirect Inhibition of BLA-vHPC Synapses

Voltage-clamp experiments in the vHPC neurons of animals expressing ChR2 in BLA neurons. Means are represented as ±SEM. See Figures S4, S7, and S8. (A) Photostimulation of BLA terminals in the vHPC trigger EPSCs and IPSCs as shown in sample traces (20 Hz, 5 ms pulses for 5 s) in a representative neuron clamped at −70 mV and 0 mV, respectively. (B) Overlay of three sample IPSCs and EPSCs; 5 ms light pulses. Bar histogram represents onset latencies, relative to the light-pulse onset. IPSC onset latencies (6.2 ± 0.85 ms) were significantly longer than EPSC latencies (3.4 ± 0.65 ms; one-tailed paired Student's t test, t = 4.430, n = 6, **p = 0.0034). (C) Overlay of three light-triggered responses during sodium and potassium channel blockade (TTX+4AP) and glutamate receptor blockade (TTX+4AP+AP5+NBXQ). Histogram represents the population analysis of current amplitudes after pharmacological manipulation. EPSCs persist under perfusion of sodium and potassium channel blockers (one-way ANOVA, $F_{2,12} = 145.4$, $p < 0.0001$, TTX+4AP in gray versus ACSF in black, Tukey post hoc analysis, ***$p < 0.001$), whereas IPSCs are abolished (TTX+4AP in gray versus ACSF in blue, one-tailed paired Student's t test, n = 5, t = 25.55, ***$p < 0.001$). GluR antags block the monosynaptic light-evoked EPSC (TTX+4AP, in gray, versus TTX+4AP+AP5+NBQX, in red, Tukey post hoc analysis, ***$p < 0.001$). (D) Model of the BLA-vHPC circuit activated in ChR2-BLA:vHPC mice. Pyramidal cells receive monosynaptic inputs from BLA, polysynaptic inputs from other pyramidal cells, and inhibition through polysynaptic mechanisms (dotted lines indicate speculated microcircuitry). "+" represents glutamatergic synapses and "−" represents GABAergic synapses.

(Figure 3B) and the OFT (Figure 3C). However, after vHPC glutamate receptor antagonism, the light-induced changes in open-arm exploration on the EPM, the time spent in the center on the OFT, and the latency to feed on the NSF test were all attenuated (Figures 3B, 3C, and 3D).

While our glutamate antagonist experiments do not rule out the possible occurrence of depolarization in axons of passage, or antidromic activation, they do demonstrate that neither of these events contributed to the light-induced anxiogenic behavioral phenomenon. Taken together, these data support the hypothesis that BLA axon terminals synapsing locally in the vHPC can bidirectionally modulate anxiety-related behaviors.

Next, we used ex vivo whole-cell patch-clamp recordings in the vHPC of mice expressing ChR2-eYFP in BLA neurons and axon terminals (Figure S7) to elucidate the local circuit mechanism in the vHPC. Given that our c-*fos* data suggested that illumination of BLA axon terminals with 20 Hz produced a strong activation of glutamatergic neurons in the pyramidal layer of the vHPC, we hypothesized that the increase in anxiety-related behaviors was mediated by a monosynaptic, direct excitation of CA1 vHPC pyramidal neurons. To test this, we used animals that underwent the same viral transduction parameters for expressing ChR2 in glutamatergic BLA neurons and took acute slices containing ChR2-expressing BLA axon terminals in the vHPC for whole-cell recordings within the CA1 pyramidal layer. Using light power density similar to those estimated at ~1.5 mm from the fiber tip, we were able to evoke robust spiking (Figures 3E and S4) and verified that these recordings were in the CA1 pyramidal cell layer by using Alexa Fluor dye in our internal pipette solution (Figures 3F and S7). Of 23 pyramidal cells recorded, we were able to obtain robust net activation across the duration of the 20 Hz train in 100% of them, in cells showing a mean resting potential of −70 mV (Figures 3D–3F and S8A). To test whether this excitation was direct (due to monosynaptic input from BLA axon terminals) or indirect (due to polysynaptic feedforward excitation), in the same cells, we perfused tetrodotoxin (TTX) and 4-amynopyridine (4AP) into the bath to remove any network activity (Petreanu et al., 2007). We observed that 89% of the pyramidal neurons we tested (17/19) received direct, monosynaptic excitatory input from BLA axon terminals, with a reduction in the amplitude of excitation. We also confirmed that these terminals were indeed releasing glutamate, as we found that the addition of AP5+NBQX abolished the light-induced excitation in these same cells (Figures 3G and 3H).

Local Circuit Mechanism Involves Direct Excitation and Indirect Inhibition of BLA-vHPC Synapses

After assessing the net effects of BLA terminal stimulation, we next wanted to parse the excitatory and inhibitory input triggered by illumination of ChR2-expressing BLA axons in the vHPC. To do this, we performed voltage-clamp recordings to isolate inhibitory postsynaptic currents (IPSCs) recorded at 0 mV and excitatory postsynaptic currents (EPSCs) recorded at −70 mV (Figure 4A). When examining the latency of time-locked IPSCs and EPSCs to the onset of each light pulse for each cell, we observed that EPSCs showed shorter onset latencies relative to IPSCs in a within-cell comparison (Figures 4B and S8E). We confirmed that EPSCs were preserved by TTX+4AP and

attenuated upon glutamate receptor antagonism. In contrast, IPSCs were not monosynaptically driven, as they were abolished by the addition of TTX and 4AP to the bath (Figure 4C). Together, these data support a model for direct (monosynaptic) excitation and indirect (polysynaptic, feedforward, and/or feedback) inhibition and also support an important role for local network activity mediated by feedforward excitation (Figure 4D).

DISCUSSION

Here, we show that bilateral inhibition of BLA axon terminals in the vHPC reduces anxiety-related behaviors, suggesting that BLA input to the vHPC is required to maintain basal levels of anxiety-related behaviors. Conversely, we found that activation of BLA axon terminals in the vHPC increases anxiety-related behaviors without inducing gross alterations of locomotor activity. Although optogenetic activation carries limitations in terms of mimicking physiological BLA activity, we speculate that the ability of photostimulation to increase anxiety-related behaviors suggests that a simpler message of unspecified threat might be transmitted by a graded response rather than a more informative patterned code as would be expected in fear conditioning to specific stimuli. However, these data do not differentiate between an instructive and permissive role of the BLA-vHPC pathway in mediating anxiety-related behaviors, and the native activity of vHPC-projecting BLA neurons during an anxiety-related task has yet to be established.

Additionally, we show that the activation of BLA inputs to the vHPC is sufficient to increase anxiety-related behaviors and that these changes are not due to backpropagating action potentials, vesicle release at distal collaterals, or depolarization of axons of passage, as the unilateral blockade of glutamate transmission in the vHPC attenuates the light-induced change in anxiety-related behavior. Furthermore, we show that BLA axon terminals provide excitatory (glutamatergic), monosynaptic input onto CA1 vHPC pyramidal neurons. Although we do observe an increase in mPFC c-*fos* after illumination of BLA terminals in the vHPC (Figure S5), consistent with previous reports that vHPC neural activity drives mPFC activity (Adhikari et al., 2010, 2011), our vHPC glutamate antagonist experiments (Figure 3) demonstrate that the BLA input to the vHPC is the neural circuit element critical for mediating the light-induced changes in anxiety-related behaviors observed here. Together, our data support a local circuit mechanism for direct excitation and indirect inhibition in the vHPC, mediated by BLA inputs.

These experiments expand the understanding of the neural underpinnings of anxiety from earlier studies examining BLA neural activity (Wang et al., 2011), microcircuitry (Tye et al., 2011), and the role of the vHPC (Adhikari et al., 2010, 2011; Bannerman et al., 2003) in anxiety-related behaviors. A recent study first demonstrated that activation of a specific BLA projection could produce opposite behavioral effects from activation of all BLA cell bodies (Tye et al., 2011), leading to the hypothesis that populations of BLA neurons projecting to different downstream targets produced opposing effects on anxiety-related behaviors and that the net effect of nonspecific activation of BLA somata was anxiogenic, while activation of BLA-CeA projections were anxiolytic. In this study, we identify and characterize the properties of the BLA-vHPC pathway, which has opposing effects on anxiety-related behaviors compared to the BLA-CeA pathway. These data demonstrate that distinct populations of intermingled neurons in the BLA projecting to different downstream targets can have unique functional properties.

With respect to the anxiety circuit as a whole, given the evolutionarily adaptive purposes of fear and anxiety for survival, it is likely that anxiety circuits are widely distributed and highly redundant. This may explain why there are a host of parallel circuits in the brain that can contribute to the modulation of anxiety states. While this study represents the identification of a projection that represents an oppositional force to existing circuits in mediating anxiety, much of the anxiety circuit has yet to be carefully characterized on a circuit and synaptic level. Other circuits to explore in the characterization of critical neural circuit elements of anxiety include the connections of the PFC, the bed nucleus of the stria terminalis, and projections from neuromodulatory regions.

EXPERIMENTAL PROCEDURES

Stereotaxic Surgery and Viral Vectors

All procedures were carried out in accordance with the guidelines from the NIH and with approval of the MIT IACUC and DCM. Adult wild-type male C57BL/6J mice (aged 5–6 weeks) were used. Purified AAV_5-CaMKIIα-eNpHR3.0-eYFP or eYFP alone was bilaterally injected for mice in Figure 1. AAV_5-CaMKIIα-ChR2-eYFP or eYFP alone was unilaterally injected for mice in Figures 2, 3, and 4. To allow for BLA-vHPC terminal photostimulation, mice received chronically implantable optical fibers aimed over the vHPC. For glutamate receptor antagonist (GluR antag) experiments, mice were unilaterally implanted with a guide cannula.

Behavioral Assays

Anxiety assays (EPM, OFT, and NSF) were performed 5–8 weeks after surgery. For in vivo pharmacology experiments, a GluR antag cocktail consisting of NBQX and AP5 dissolved in saline was injected into vHPC 30 min before the behavioral assays and optogenetic manipulations. For mice in Figure 1, ~10 mW of constant yellow light was bilaterally delivered onto BLA-vHPC terminals. For mice injected with ChR2 or eYFP control in the BLA (Figures 2 and 3), 10–15 mW of light at 20 Hz, 5 ms pulses of blue light was delivered unilaterally onto BLA-vHPC terminals.

Immunohistochemistry and Confocal Microscopy

Mice included in Figure 2 (ChR2 and eYFP) were stimulated with 473 nm laser and perfused 90 min after and the brain was extracted for c-*fos* expression quantification. Primary antibody (1:500) was incubated for 17–20 hr at 4°C. Sections were then washed with PBS-1X prior to and after incubation with secondary antibody (Alexa Flour 647 1:500) for 2 hr at 25°C. Sections were then incubated with a DNA-specific fluorescent probe (1:50,000) for 30 min and slide mounted with PVD-DABCO. C-fos-positive cells were quantified through z stack projections by experimenters blind to the experimental conditions.

Ex Vivo Electrophysiology

Coronal sections of 300 μm containing the vHPC were collected. Whole-cell patch-clamp recordings were made from visually identified pyramidal neurons in the CA1 region of the vHPC. BLA terminals expressing ChR2 were activated using a 470 nm LED. Amplitudes and onset latencies of postsynaptic potentials and currents were measured for the first pulse (Figure 4) and for the average response of each neuron (Figure S8).

Statistical Analysis

Group differences were detected using either one-way ANOVA with Tukey's post hoc tests or two-way repeated-measures ANOVA with Bonferroni post hoc tests. Paired statistical comparisons were made with a one-tailed paired

Student's t test. For all results, significativity threshold was placed at p = 0.05. All data are shown as ±SEM.

SUPPLEMENTAL INFORMATION

Supplemental Information includes Supplemental Experimental Procedures, eight figures, and three movies and can be found with this article online at http://dx.doi.org/10.1016/j.neuron.2013.06.016.

ACKNOWLEDGMENTS

We thank P. Namburi for sharing the cell-counting software, K. Kohara for the biocytin-streptavidin protocol, and all members of the Tye Laboratory for their helpful discussion. We would like to thank M. Dobbins, L.-H. Tsai, K. Jones, W. Xu, Q. Zhang, and G. Feng for providing access to their confocal microscopes. We acknowledge Dr. R.J. Samulski and the UNC Vector Core for gene transfer vectors preparation. This work was supported by funds from the JPB Foundation, Picower Institute Innovation Funds, The Whitehall Foundation, The Klingenstein Foundation, and startup funds provided by the Picower Institute for Learning and Memory and the Department of Brain and Cognitive Sciences at MIT (K.M.T). A.B. was supported by a postdoctoral fellowship for prospective researchers from the Swiss National Science Foundation (SNSF; Project number: PBSKP3_143586). C.A.L. was supported by the MIT Summer Research Program and by HHMI undergraduate education grant.

Accepted: June 6, 2013
Published: August 21, 2013

REFERENCES

Adamec, R.E., Burton, P., Shallow, T., and Budgell, J. (1999). Unilateral block of NMDA receptors in the amygdala prevents predator stress-induced lasting increases in anxiety-like behavior and unconditioned startle—effective hemisphere depends on the behavior. Physiol. Behav. *65*, 739–751.

Adhikari, A., Topiwala, M.A., and Gordon, J.A. (2010). Synchronized activity between the ventral hippocampus and the medial prefrontal cortex during anxiety. Neuron *65*, 257–269.

Adhikari, A., Topiwala, M.A., and Gordon, J.A. (2011). Single units in the medial prefrontal cortex with anxiety-related firing patterns are preferentially influenced by ventral hippocampal activity. Neuron *71*, 898–910.

Bannerman, D.M., Grubb, M., Deacon, R.M., Yee, B.K., Feldon, J., and Rawlins, J.N. (2003). Ventral hippocampal lesions affect anxiety but not spatial learning. Behav. Brain Res. *139*, 197–213.

Büchel, C., Dolan, R.J., Armony, J.L., and Friston, K.J. (1999). Amygdala-hippocampal involvement in human aversive trace conditioning revealed through event-related functional magnetic resonance imaging. J. Neurosci. *19*, 10869–10876.

Carola, V., D'Olimpio, F., Brunamonti, E., Mangia, F., and Renzi, P. (2002). Evaluation of the elevated plus-maze and open-field tests for the assessment of anxiety-related behaviour in inbred mice. Behav. Brain Res. *134*, 49–57.

Ciocchi, S., Herry, C., Grenier, F., Wolff, S.B.E., Letzkus, J.J., Vlachos, I., Ehrlich, I., Sprengel, R., Deisseroth, K., Stadler, M.B., et al. (2010). Encoding of conditioned fear in central amygdala inhibitory circuits. Nature *468*, 277–282.

Davidson, R.J. (2002). Anxiety and affective style: role of prefrontal cortex and amygdala. Biol. Psychiatry *51*, 68–80.

Etkin, A., Prater, K.E., Schatzberg, A.F., Menon, V., and Greicius, M.D. (2009). Disrupted amygdalar subregion functional connectivity and evidence of a compensatory network in generalized anxiety disorder. Arch. Gen. Psychiatry *66*, 1361–1372.

File, S.E., and Gonzalez, L.E. (1996). Anxiolytic effects in the plus-maze of 5-HT1A-receptor ligands in dorsal raphé and ventral hippocampus. Pharmacol. Biochem. Behav. *54*, 123–128.

Gradinaru, V., Zhang, F., Ramakrishnan, C., Mattis, J., Prakash, R., Diester, I., Goshen, I., Thompson, K.R., and Deisseroth, K. (2010). Molecular and cellular approaches for diversifying and extending optogenetics. Cell *141*, 154–165.

Han, J.-H., Kushner, S.A., Yiu, A.P., Hsiang, H.-L., Buch, T., Waisman, A., Bontempi, B., Neve, R.L., Frankland, P.W., and Josselyn, S.A. (2009). Selective erasure of a fear memory. Science *323*, 1492–1496.

Haubensak, W., Kunwar, P.S., Cai, H., Ciocchi, S., Wall, N.R., Ponnusamy, R., Biag, J., Dong, H.-W., Deisseroth, K., Callaway, E.M., et al. (2010). Genetic dissection of an amygdala microcircuit that gates conditioned fear. Nature *468*, 270–276.

Kheirbek, M.A., Drew, L.J., Burghardt, N.S., Costantini, D.O., Tannenholz, L., Ahmari, S.E., Zeng, H., Fenton, A.A., and Hen, R. (2013). Differential control of learning and anxiety along the dorsoventral axis of the dentate gyrus. Neuron *77*, 955–968.

Kjelstrup, K.G., Tuvnes, F.A., Steffenach, H.A., Murison, R., Moser, E.I., and Moser, M.B. (2002). Reduced fear expression after lesions of the ventral hippocampus. Proc. Natl. Acad. Sci. USA *99*, 10825–10830.

McHugh, S.B., Deacon, R.M.J., Rawlins, J.N.P., and Bannerman, D.M. (2004). Amygdala and ventral hippocampus contribute differentially to mechanisms of fear and anxiety. Behav. Neurosci. *118*, 63–78.

O'Donnell, P., and Grace, A.A. (1995). Synaptic interactions among excitatory afferents to nucleus accumbens neurons: hippocampal gating of prefrontal cortical input. J. Neurosci. *15*, 3622–3639.

Paton, J.J., Belova, M.A., Morrison, S.E., and Salzman, C.D. (2006). The primate amygdala represents the positive and negative value of visual stimuli during learning. Nature *439*, 865–870.

Petreanu, L., Huber, D., Sobczyk, A., and Svoboda, K. (2007). Channelrhodopsin-2-assisted circuit mapping of long-range callosal projections. Nat. Neurosci. *10*, 663–668.

Pikkarainen, M., Rönkkö, S., Savander, V., Insausti, R., and Pitkänen, A. (1999). Projections from the lateral, basal, and accessory basal nuclei of the amygdala to the hippocampal formation in rat. J. Comp. Neurol. *403*, 229–260.

Pitkänen, A., Stefanacci, L., Farb, C.R., Go, G.-G., LeDoux, J.E., and Amaral, D.G. (1995). Intrinsic connections of the rat amygdaloid complex: projections originating in the lateral nucleus. J. Comp. Neurol. *356*, 288–310.

Richardson, M.P., Strange, B.A., and Dolan, R.J. (2004). Encoding of emotional memories depends on amygdala and hippocampus and their interactions. Nat. Neurosci. *7*, 278–285.

Somerville, L.H., Kim, H., Johnstone, T., Alexander, A.L., and Whalen, P.J. (2004). Human amygdala responses during presentation of happy and neutral faces: correlations with state anxiety. Biol. Psychiatry *55*, 897–903.

Tye, K.M., and Deisseroth, K. (2012). Optogenetic investigation of neural circuits underlying brain disease in animal models. Nat. Rev. Neurosci. *13*, 251–266.

Tye, K.M., Cone, J.J., Schairer, W.W., and Janak, P.H. (2010). Amygdala neural encoding of the absence of reward during extinction. J. Neurosci. *30*, 116–125.

Tye, K.M., Prakash, R., Kim, S.-Y., Fenno, L.E., Grosenick, L., Zarabi, H., Thompson, K.R., Gradinaru, V., Ramakrishnan, C., and Deisseroth, K. (2011). Amygdala circuitry mediating reversible and bidirectional control of anxiety. Nature *471*, 358–362.

Wang, D.V., Wang, F., Liu, J., Zhang, L., Wang, Z., and Lin, L. (2011). Neurons in the amygdala with response-selectivity for anxiety in two ethologically based tests. PLoS ONE *6*, e18739.